Cytidine Deaminases from *B. subtilis* and *E. coli*: Compensating Effects of Changing Zinc Coordination and Quaternary Structure†

Dean C. Carlow,‡ Charles W. Carter, Jr.,‡ Nina Mejlhede,§ Jan Neuhard,§ and Richard Wolfenden*,‡

Department of Biochemistry and Biophysics, University of North Carolina, Chapel Hill, North Carolina 27599-7260, and Center for Enzyme Research, Institute of Molecular Biology, University of Copenhagen, Copenhagen, Denmark

Received April 8, 1999; Revised Manuscript Received July 21, 1999

ABSTRACT: Cytidine deaminase from *E. coli* is a dimer of identical subunits ($M_r = 31\,540$), each containing a single zinc atom. Cytidine deaminase from *B. subtilis* is a tetramer of identical subunits ($M_r = 14\,800$). After purification from an overexpressing strain, the enzyme from *B. subtilis* is found to contain a single atom of zinc per enzyme subunit by flame atomic absorption spectroscopy. Fluorescence titration indicates that each of the four subunits contains a binding site for the transition state analogue inhibitor 5-fluoro-3,4-dihydrouridine. A region of amino acid sequence homology, containing residues that are involved in zinc coordination in the enzyme from *E. coli*, strongly suggests that in the enzyme from *B. subtilis*, zinc is coordinated by the thiolate side chains of three cysteine residues (Cys-53, Cys-86, and Cys-89) [Song, B. H., and Neuhard, J. (1989) *Mol. Gen. Genet. 216*, 462−468]. This pattern of zinc coordination appears to be novel for a hydrolytic enzyme, and might be expected to reduce the reactivity of the active site substantially compared with that of the enzyme from *E. coli* (His-102, Cys-129, and Cys-132). Instead, the *B. subtilis* and *E. coli* enzymes are found to be similar in their activities, and also in their relative binding affinities for a series of structurally related inhibitors with binding affinities that span a range of 6 orders of magnitude. In addition, the apparent pK_a value of the active site is shifted upward by less than 1 unit. Sequence alignments, together with model building, suggest one possible mechanism of compensation.

Cytidine deaminase from *E. coli* is a dimeric protein that contains one atom of tightly bound zinc in each subunit (*1*, *2*) (Figure 1). The three-dimensional structure of this enzyme's complex with the transition state analogue inhibitor 3,4-dihydrouridine ($K_i = 1.2 \times 10^{-12}$ M) shows that the zinc atom lies deeply buried within the active site, where it is coordinated by a nitrogen atom of His-102 and by the thiolate groups of Cys-129 and Cys-132 (*2*). In an environment that is sequestered almost completely from bulk solvent, this zinc atom appears to activate substrate water for attack on the pyrimidine ring, in conjunction with the carboxylate group of Glu-104 (*2*, *3*). Replacement of any of these zinc-coordinating residues by alanine results in major losses in the enzyme's affinity for zinc, and also in its catalytic activity (*4*).

In other zinc-containing hydrolases and hydratases, catalytic zinc atoms are usually ligated by histidine (as in carbonic anhydrase and adenosine deaminase, with three His residues), and also, less frequently, by carboxylate groups (as in carboxypeptidase A, with two His residues and one Glu residue) (for reviews, see *5* and *6*), with water or a hydroxide ion occupying the fourth coordination position. In this respect, the coordination motif of *E. coli* cytidine deaminase (with one His residue and two Cys residues) appears to be unusual among hydrolytic enzymes, although it is also found in some other deaminases that act on cytosine derivatives, in deoxycytidylate deaminase, and in a recently discovered mRNA-editing enzyme from mammals, apobec-1 (*7*).

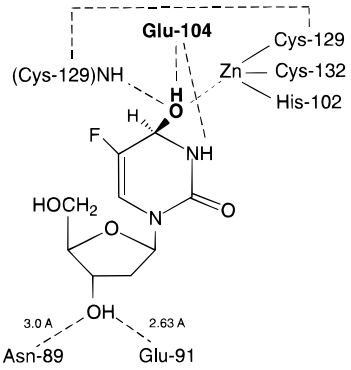

FIGURE 1: Active site of *E. coli* cytidine deaminase, showing enzyme interactions with the transition-state analogue 5-fluoro-3,4-dihydrouridine that have been inferred from the crystal structure of the CDA−FZEB complex (*2*).

In the small, tetrameric cytidine deaminases of *B. subtilis* (*8*) and of humans (*9*, *10*), a cysteine residue is found at the position corresponding to the histidine residue in the first part of the zinc-binding motif of *E. coli* cytidine deaminase (Figure 2). The apparent involvement of three cysteine residues in zinc coordination, although common for "structural" zinc atoms in proteins, appears to be unprecedented at the active site of a hydrolytic enzyme. Moreover,

† This research was supported by Grant GM18325 from the National Institutes of Health.

* To whom correspondence should be addressed. Fax: (919)-962-2852. E-mail: water@med.unc.edu.

‡ University of North Carolina.

§ University of Copenhagen.

10.1021/bi990819t CCC: $18.00
Published on Web 09/01/1999

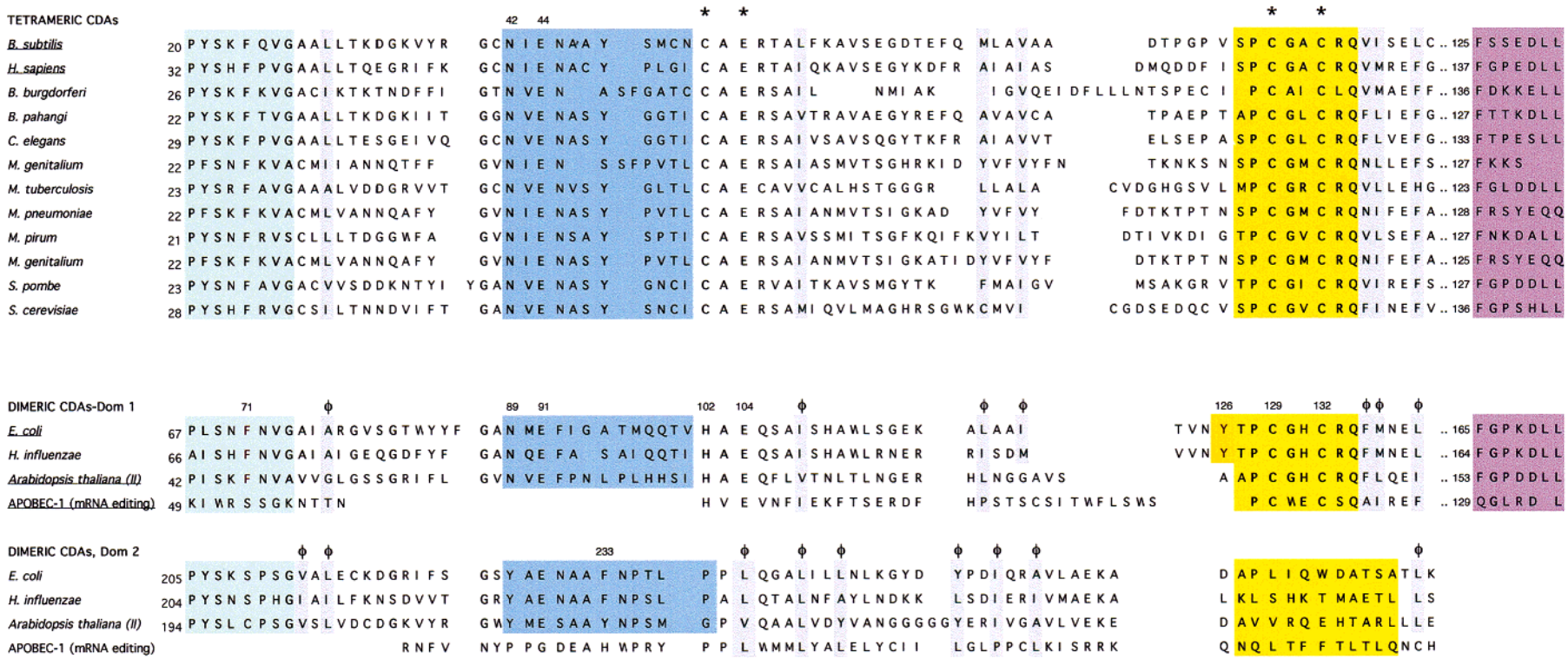

FIGURE 2: Comparative alignment of amino acid sequences for tetrameric and dimeric cytidine deaminases. Consensus motifs are in boldface. Probable zinc ligands are indicated by asterisks. Enzymes proven to contain zinc are underlined. Sequences were obtained through the ExPASy interface to the SWISS-PROT database. Thematic sequence elements are colored to assist the interpretation of Table 2 and Figure 6 as follows: Segments forming the dimer interface in dimeric CDAs are shaded green, blue, yellow, and red in the order in which they occur in the sequences of the tetrameric CDA subunits (Figure 6) and the two core domains of the dimeric CDAs. Residues contributing to the principal hydrophobic core region, as identified in ref *2*, are shaded light gray and indicated by ϕ to emphasize the similarity between their patterns in the tetrameric CDAs and in the first core domain of the dimeric CDAs.

coordination of zinc by three cysteine residues appears to be strictly correlated with a tetrameric quaternary structure in these deaminases (Figure 2).

In the present work, we confirm that the enzyme from *B. subtilis* contains zinc, and compare its stoichiometry with the stoichiometry of binding of the transition state analogue inhibitor 5-fluoro-3,4-dihydrouridine. The results indicate that a single active site, containing a catalytic zinc atom coordinated by three protein thiolate groups, is present in each enzyme subunit (M_r = 14 800). The four subunits appear to be identical and independent in their binding behavior, as indicated by fluorescence titration. The enzymes from *B. subtilis* and *E. coli*, although they differ markedly in the number of subunits and patterns of zinc coordination, are shown to be remarkably similar in their active site pK_a values, and in their relative binding affinities for a set of structurally related analogue inhibitors whose individual binding affinities differ by 6 orders of magnitude. These inhibitors allow comparison of the binding contributions of functional groups of these ligands, in the different settings provided by the active sites of the two enzymes.

MATERIALS AND METHODS

Materials. Cytidine deaminase was purified from *E. coli* SØ268 harboring plasmid pSO143. This plasmid contains the *B. subtilis* cytidine deaminase gene cloned behind the *E. coli lac* promoter of pUC19 (*8*). Cells were grown with vigorous aeration at 37 °C in L broth (*11*) supplemented with ampicillin (200 mg/L) for 16 h, and then harvested by centrifugation to yield 18 g of cell paste. Cells were then suspended in 70 mL of buffer A (Tris-HCl, 0.1 M, pH 7.6) and sonicated, and the cell debris were removed by centrifugation. Nucleic acids were removed by precipitation with streptomycin sulfate (1%), and the supernatant was applied to a column of DEAE-cellulose (DE-52, 2.5 × 30 cm) equilibrated with buffer A. After the column was washed with buffer A (300 mL), enzyme activity was eluted with a gradient (900 mL) from 0.0 to 0.3 M NaCl in buffer A in the cold, using a flow rate of 2 mL/min. Active fractions were pooled (150 mL), and then adjusted to 60% saturation with ammonium sulfate. The precipitate, obtained by centrifugation, was redissolved in buffer B (Tris-HCl, 0.05 M, pH 7.6) and dialyzed against buffer B. The dialyzed solution was heated to 68 °C for 10 min, and then cooled rapidly. The precipitate was removed by centrifugation, and the supernatant was applied to a gel filtration column (Sephadex G-75, 2.5 × 90 cm) equilibrated with buffer B. The enzyme was eluted with buffer B at a flow rate of 0.5 mL/min. Active fractions were applied to a Bio-Rad Q5 column equilibrated with buffer C (Tris-HCl, 0.02 M, pH 7.6), and the enzyme was eluted with a gradient (50 mL) from 0.0 to 0.5 M KCl, in buffer C. Active fractions were pooled and concentrated by ultrafiltration in a Centriprep tube (Amicon, Inc.). The resulting protein was >98% pure as judged by SDS−PAGE. The progress of a typical preparation is shown in Table 1. The final specific activity (238 units/mg) is comparable in magnitude with that reported earlier (570 units/mg) for the enzyme from *E. coli* (*4*).

Table 1: Purification of *B. subtilis* Cytidine Deaminase

purification step	mL	mg	units	units/mg	fold	% yield
crude extract	80	2640	94500	36	1	100
streptomycin	86	2494	87000	35	1	92
DEAE	15.3	421	42000	100	2.8	44
heat denaturation	12.1	290	35800	123	3.4	38
G-75	35	228	44000	193	5.4	47
Q5	3	63	15000	238	6.6	16

The inhibitors zebularine (ZEB),[1] 5-fluorozebularine (FZEB), and 3,4-dihydrozebularine (II) were gifts from Dr. Victor Marquez (National Cancer Institute, NIH, Bethesda, MD). 3,4,5,6-Tetrahydrouridine [1-(β-D-ribofuranosyl)-4-hydroxytetrahydro-2(1*H*)-pyrimidone] (III) and 3,4,5,6-tetrahydrozebularine [1-(β-D-ribofuranosyl)tetrahydro-2(1*H*)-pyrimidone] (IV) were synthesized according to the method of Hanze (*12*).

Determination of the Dissociation Constant of 5-Fluorozebularine. The binding of FZEB was observed by quenching of this inhibitor's fluorescence as described earlier (*13*) with a Hitachi F-2000 spectrofluorometer thermostated at 25 ± 0.1 °C, using a 3 mL cuvette (1-cm light path). In these experiments, FZEB and protein were present at concentrations between 5×10^{-8} and 1×10^{-5} M, at which the absorbencies of both partners amounted to less than 0.04 at the wavelength (322 nm) of excitation. The fluorescence of FZEB was quenched approximately 73% upon binding by the *B. subtilis* protein, similar to the quenching observed earlier using the enzyme from *E. coli*. To determine the dissociation constant, a solution of FZEB (6.6×10^{-8} M) was titrated with enzyme, in potassium phosphate buffer (25 mM, pH 7.0). Because FZEB is bound very tightly, it was necessary to correct for depletion of the free enzyme. The concentration of free enzyme, $[E]_{free}$, was calculated according to the equation:

$$[E]_{free} = [E]_{total} - (\Delta F/\Delta F_{max})[FZEB]$$

in which ΔF is the observed fluorescence change, ΔF_{max} is the total fluorescence quenching at saturating binding sites, and [FZEB] is the concentration of FZEB. Dissociation constants were determined by nonlinear regression analysis of a plot of the change in the relative fluorescence, ΔF, as a function of the concentration of free enzyme.

Enzyme Assay. The deamination of cytidine in potassium phosphate buffer (0.1 M, pH 7.0) was monitored at 282 nm ($\Delta\epsilon_M = -3600$) using cuvettes maintained at 25 °C (*14*). Inhibitor dissociation constants were determined from double reciprocal plots of enzyme activity as a function of changing substrate concentration in the presence and absence of inhibitors. The K_i values reported in Figure 5 represent the mean of six experimental determinations.

Zinc Analysis. Buffers were treated with Chelex-100 resin (Bio-Rad, Richmond, CA) (*15*). Glassware and polyethylene containers were rendered metal-free by soaking overnight in a 1:1 mixture of concentrated nitric and sulfuric acids (*16*). Dialysis tubing was freed of metal ions as described by Auld (*17*). The quantity of enzyme in each dialyzed sample was determined using the Coomassie protein assay (Bio-Rad, Richmond, CA), with bovine serum albumin as a standard. Before metal analysis, excess and loosely associated metal ions were removed by prolonged dialysis against metal-free

[1] Abbreviations: CDA, cytidine deaminase; ZEB, zebularine; FZEB, 5-fluorozebularine; 3,4-hydrate of FZEB, 3,4-dihydro-5-fluoropyrimidin-2-one ribonucleoside or 5-fluoro-3,4-dihydrouridine.

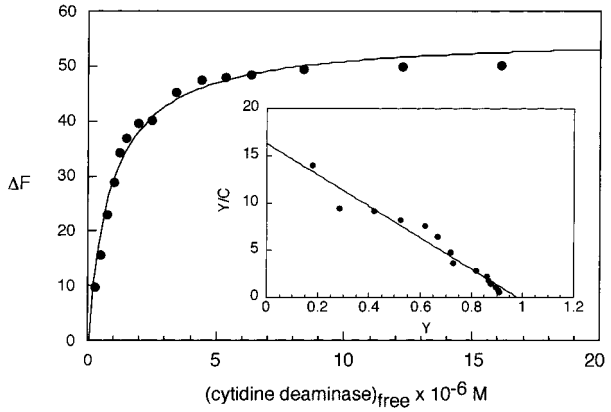

FIGURE 3: Decreases in fluorescence intensity that accompany the binding of FZEB (6.6×10^{-8} M) by cytidine deaminase from *B. subtilis*. The Scatchard plot (inset) shows that the enzyme has one FZEB binding site per enzyme subunit (M_r 14 800). *Y* is the fraction of enzyme bound to FZEB, and *C* is the concentration of free enzyme subunits (μM).

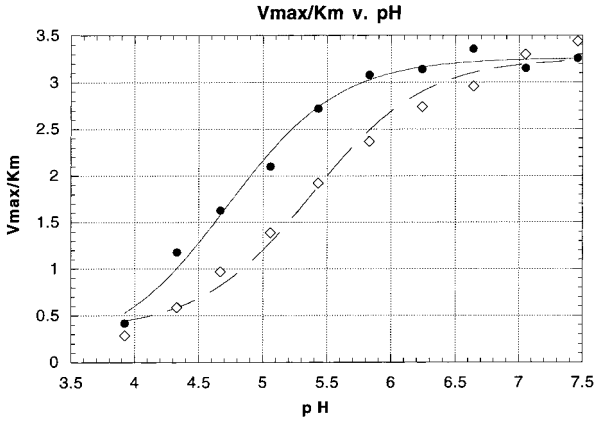

FIGURE 4: Values of k_{cat}/K_m for cytidine deaminase from *E. coli* (circles) and *B. subtilis* (diamonds), plotted as a function of pH. The lines are theoretical curves based on assumed pK_a values of 4.7 for the *E. coli* enzyme and 5.4 for the *B. subtilis* enzyme.

HEPES-HCl buffer (10 mM, pH 7.0). The specific activity of the enzyme, determined before and after dialysis, was 226 $\pm$ 6 units/mg, indicating that essential zinc atoms had not been lost during dialysis. Samples of enzyme were analyzed for zinc content using an Instrumentation Laboratories S-12 flame atomic absorption spectrometer.

Influences of pH on k_{cat}/K_m. Influences of pH on k_{cat}/K_m were determined for both enzymes in the presence of potassium acetate buffers (0.02 M) in the pH range between 3.8 and 5.4 and potassium phosphate buffers (0.02 M) in the pH range between 5.8 and 7.5. The reaction was monitored at 290 nm, by the disappearance of 2′-deoxycytidine (2×10^{-5} M), using cuvettes maintained at 23 °C. Rate calculations were based on $\Delta\epsilon_M$ values that varied from -7.49×10^3 at pH 3.9 to -1.69×10^3 at pH 7.5, with a pK_a value of 4.2 (*18*).

RESULTS

Enzyme Inhibition. The results of the present study are shown in Figure 5, along with some K_i values previously determined for the enzyme from *E. coli* (*19*). Each of the inhibitors showed competitive inhibition, as indicated by double reciprocal plots of enzyme activity as a function of changing substrate concentration. Enzyme assays performed before and after preincubation of enzymes with inhibitors showed no evidence of time-dependent inactivation. These inhibitors were chosen because of their wide variation in affinity as a means of assessing the equilibrium binding properties of the active site, including its zinc atom, that are believed to contribute to catalysis (see Discussion).

Zinc Analysis. Analysis for zinc using flame atomic absorption spectroscopy revealed the presence of 1.13 ± 0.05 tightly bound zinc atoms per enzyme subunit (14 800 Da). The specific activity of the enzyme remained constant during the prolonged "metal-free" dialysis, suggesting that no metal atoms essential for catalysis were removed by this procedure.

Binding of 5-Fluorozebularine. Figure 3 shows changes in fluorescence intensity (ΔF) that were observed upon addition of the enzyme from *B. subtilis* to a solution of FZEB. As in the case of the enzyme from *E. coli* (*13*), the binding of FZEB by the enzyme from *B. subtilis* is accompanied by quenching of the inhibitor's fluorescence, and to virtually the same extent. After correction for the amount of enzyme bound by the ligand, plots of ΔF as a function of the concentration of free enzyme were hyperbolic. High concentrations of the substrate cytidine were found to displace FZEB from the active site of the enzyme, as indicated by the reappearance of fluorescence, showing that FZEB competes with substrate for a place on the enzyme. The dissociation constant of FZEB from the enzyme from *B. subtilis*, in the absence of substrate, is 5.4×10^{-8} M as indicated by nonlinear regression analysis. Thus, the enzyme from *B. subtilis* binds FZEB approximately 2-fold more tightly than does the enzyme from *E. coli*.

The dissociation constant of the complex formed between the enzyme from *B. subtilis* and the covalent 3,4-hydrate of FZEB (3,4-dihydro-5-fluoropyrimidin-2-one ribonucleoside), estimated as the product of its dissociation constant and the equilibrium constant for 3,4-hydration of FZEB as described earlier (*13*), was 1.9×10^{-11} M, slightly lower than the value of 3.9×10^{-11} M previously observed for the enzyme from *E. coli*. Figure 5 shows that although the enzyme from *B. subtilis* binds 5-fluorozebularine more tightly than does the enzyme from *E. coli* enzyme, it binds the unfluorinated inhibitor zebularine 6.8-fold less tightly than does the *E. coli* enzyme.

The data in Figure 3 (inset) are also shown as a Scatchard plot, in which *Y* is the fraction of enzyme bound to FZEB and *C* is the concentration of free enzyme (micromolar). Each protein subunit (M_r 14 800) binds approximately one molecule of FZEB, as shown by the intercept on the abscissa. The linearity of this plot indicates that the binding sites function independently of each other, in agreement with earlier results that failed to detect allosteric behavior from kinetic profiles (N. Mejlhede, unpublished results).

pK_a Values of B. subtilis and E. coli Cytidine Deaminases. Figure 4 shows the influence of pH on enzyme activity at low substrate concentration. These curves indicate that both enzymes are inactive at low pH, with apparent pK_a values of 4.7 for the *E. coli* enzyme and 5.4 for the *B. subtilis* enzyme.

DISCUSSION

Comparison of Properties. This work has shown that cytidine deaminase from *B. subtilis*, like the enzyme from

E. coli, contains one atom of Zn per subunit. Fluorescence titration indicates that each of its four subunits contains a binding site for the transition state analogue inhibitor 5-fluoro-3,4-dihydrouridine. A region of amino acid sequence homology, containing residues that are involved in zinc coordination in the enzyme from *E. coli*, strongly suggests that in the enzyme from *B. subtilis*, zinc is coordinated by the thiolate side chains of three cysteine residues (Cys-53, Cys-86, and Cys-89) (*8*).

The three-cysteine pattern of zinc coordination in cytidine deaminase from *B. subtilis* does not appear to have been described before for any hydrolytic enzyme, although it has been reported for the catalytic zinc atom of cobalamin-independent methionine synthase (*20*). In the absence of other differences, substitution of a sulfur ligand for a histidine nitrogen ligand might have been expected to depress reactivity. Bertini and co-workers have carried out a series of molecular orbital calculations for Zn(N3)OH, Zn(N2)(S)-OH, and Zn(N)(S2)(OH) complexes, and their results show a qualitative trend toward higher pK_a values as the nitrogen ligands are replaced by sulfur ligands (*21*). In accord with these calculations, mutagenesis experiments performed on carbonic anhydrase demonstrated the importance of neutral ligands in maintaining the low pK_a of zinc-bound water molecules (*22*, *23*) This catalytic zinc atom is coordinated by three histidine residues and a hydroxide ion in tetrahedral geometry. Substitution of one of these His ligands with a negatively charged Cys thiolate or Asp carboxylate increased the pK_a of the zinc-bound water up to 2.7 pH units, and crystal structures of these variants demonstrated that the engineered zinc ligands coordinated the zinc atom with optimal stereochemistry (*24*). This work suggests that the electrostatic environment around the zinc site modulates the pK_a of zinc-bound water with an increasing negative charge on the zinc ion correlating directly with an increased pK_a of the zinc-bound water molecule.

The present results indicate that the steady-state catalytic activity of the enzyme from *B. subtilis* and its relative binding affinities for several 2-ketopyrimidine nucleoside inhibitors that differ from each other in the presence or absence of a 4-OH group or of unsaturation at the 5,6 position are similar to those properties of the enzyme from *E. coli* (Figure 5). In the *B. subtilis* enzyme, the active site's apparent pK_a is shifted upward from ~4.7 to ~5.4, as indicated by a plot of log (k_{cat}/K_m) vs pH (Figure 4), in the direction expected from the negative charge of the third coordinating cysteine residue.

At present, we do not have information that would exclude the possibility that the steady-state catalytic activities of these enzymes are controlled, at least in part, by a physical event such as substrate binding or product release. In that case, minor differences between these enzymes in the steady-state activity and its pH dependence (Figure 4) could mask larger differences that might be present in the individual chemical steps of catalysis. Nor can we exclude the possibility that the apparent pK_a values indicated by the inflection in Figure 4 might actually represent changes in the rate-determining step. These potential complications of interpretation do not arise in considering the behavior of the competitive inhibitors shown in Figure 5, whose K_i values represent equilibrium binding affinities.

Figure 5 shows that the equilibrium binding free energies implied by the inhibition constants for the four inhibitors

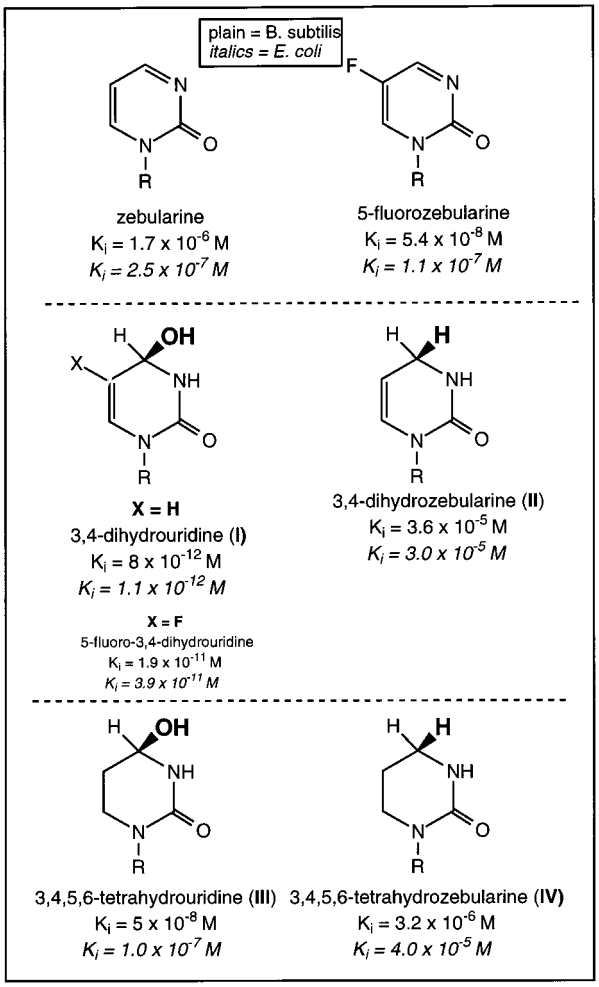

FIGURE 5: Structures of the inhibitors used in this study, and their K_i values for *B. subtilis* cytidine deaminase. Values for *E. coli* cytidine deaminase are shown in italic.

are roughly the same in the enzymes from both sources. Of particular interest are those features, the 4-OH group coordinated by zinc and by Glu-104 (Figure 1) and the unsaturated 5,6 double bond, that distinguish transition state from ground state binding. The relative contributions of these two structural features and their synergism are expressed to almost exactly the same degree in binding by both enzymes. The 5,6 double bond is much more important to the binding affinity of the OH-containing inhibitors (~10^4-fold; compare I with III) than it is to the binding of the H-containing inhibitors (~10-fold; compare II with IV). Since this effect is expressed to nearly the same extent in the enzymes from *E. coli* and *B. subtilis*, we infer that the source of the enzyme, and hence the differences in zinc atom coordination, does not significantly contribute to its response to changes in the detailed configurations of these inhibitors and the disposition of their binding determinants.

In summary, a fundamental change in zinc coordination appears to have little effect on the functional properties of cytidine deaminase, even though the enzyme's activity shows exquisite sensitivity to apparent minor changes in the structures of substrates and inhibitors as shown, for example, in Figure 5. Evidently the change from His to Cys, involved in the present comparison of enzymes from *E. coli* and *B. subtilis*, is compensated by other changes in structure. How might such compensation occur? Before considering that

Table 2: Dimer Interface and Composite Active Site Construction in *E. coli* CDA[a]

residues	68−71	91−102	127−134	159−170	206−207	227−238	268−278
buried surface (Å^2)	125	481	308	363	31	350	271
% of total area	6	25	16	19	2	18	14
active site residues	F71	E91	(Y126)	F165		F233	
		H102	P128	L170			
		(E104)	C129				
			C132				

[a]The entire dimer interface in *E. coli* CDA is constructed from 3 short loops from each core domain, together with an 11 residue stretch of the linker between them. Active site residues that do not contribute directly to the dimer interface are identified by parentheses. The linker between the first and second core domains occurs between residue 159 and 170.

question, it is of interest to compare the overall tertiary and quaternary structures of the two enzymes.

Quaternary Interactions and the Composite Active Site. Comparison of amino acid sequences of tetrameric and dimeric cytidine deaminases (Figure 2) shows the presence of numerous identities. The 32 kDa monomers of the *E. coli* enzyme are each composed of two very similar core domains. Only one of these, which we will designate the first domain, contains zinc. However, both the first and second domains are of nearly the same size as the four identical subunits of the tetrameric cytidine deaminases (Figures 5 and 7 of ref *2*). These small core domains are arranged with approximate *222* symmetry (*2*). That symmetry is also expected for a tetrameric enzyme containing four equivalent subunits. Significantly, the *E. coli* enzyme's binding sites are composite, receiving contributions from each of the two subunits. Betts et al. (Figure 11 of ref *2*) identified three kinds of active site binding determinants, in addition to those directly involved with the activated hydroxyl group. Those include residues forming a loop with hydrogen bonds to ribose (N89 and E91), four aromatic side chains that interact with the pyrimidine (F71, Y126, F165, and F233), and the residue P128 which constrains the leaving ammonia binding site.

The *E. coli* dimer interface consists of seven segments detailed in Table 2. Three of these arise from the first core domain and three others from corresponding segments in the second core domain. They are shaded green, blue, and yellow, respectively, in Figure 2. The seventh (central) segment is from the linker between the two core domains and is shaded red in Figure 2. Clearly these segments share a high proportion of identical and highly conserved amino acids between the dimeric CDAs. As noted in Table 2, row 4, all active site residues in *E. coli* CDA arise from these segments. Residues F165, F233, and L170, a residue not previously noted (*2*), are provided in trans (that is, by the second monomer across the dimer interface).

Based on the observed sequence identities (Figure 2), the tetrameric *B. subtilis* enzyme sequences might provide, in cis (i.e., from within the same monomer), residues corresponding to N89, E91 (N42, E44), to F71 (F24), and to P128 (P85). If these residues have the same spatial arrangement in both enzymes, then it seems reasonable to suppose that the four *B. subtilis* subunits adopt an overall fold like those of the small core domains in the *E. coli* enzyme.

The dual roles of F165 and L170 in forming the dimer interface and the composite active site have been noted in Table 2. Residue Q134 participates in an intimate hydrogen bond across the interface to the amide nitrogen of G130 from the other monomer. The strict conservation of the corresponding *B. subtilis* residues F125, L130, and Q91 provides substantial evidence that these residues serve similar dual roles in the tetrameric enzymes. The absence of the second core domain in the tetrameric subunit, together with the absence of tyrosine in the position homologous to Y126, suggests that the functional roles of aromatic side chains Y126 and F233 in the *E. coli* enzyme are provided in trans, by interactions involving a third subunit in the tetramer.

The tetrameric cytidine deaminases contain two highly conserved tyrosine residues not found in any of the dimeric cytidine deaminase sequences. One of these, Y48, is in the presumptive ribose binding loop that also contains N42 and E44, corresponding to N89 and E91 in the *E. coli* active site (Figure 1). That loop is structurally homologous to a loop that contains F233 in the second domain of the *E. coli* enzyme. The second tyrosine residue occurs in the sequence P20-Y21-S22, which is conserved in the zinc-containing domain of the *E. coli* enzyme (P67-L68-S69) and is identical to a sequence in the structurally homologous loop in the second, non-zinc-containing, domain (P205-Y206-S207). The quaternary structure of the *B. subtilis* enzyme, and of other tetrameric cytidine deaminases, might thus be approximated by two steps, diagrammed in Figure 6:

1. Maintain the interface contacts between first domains of the two monomers in the *E. coli* enzyme, providing the function of F165 (red) to the active site.

2. Align two copies of this dimer by superimposing loops 67−69 (green) and 91−95 (blue) from the *E. coli* enzyme first domain onto the structurally homologous sequences 205−207 (green) and 228−223 (blue) of the *E. coli* second domain, preserving *222* symmetry and providing the conserved tyrosines to the active site, in trans, across the resulting tetrameric interface. That superposition appears to produce a plausible tetrameric structure, whose relevant interface is illustrated in Figure 6.

Structural Compensations for 3-Cysteine Coordination. As noted earlier, a fundamental change in zinc coordination appears to have little effect on the functional properties of cytidine deaminase, even though the enzyme's activity is highly sensitive to changes in ligand structure. Substitution of the cysteine thiolate for the imidazole nitrogen of histidine in the tetrameric enzyme is likely to result in increased electron donation to zinc, thereby reducing its ability to activate water. Evidently the change is compensated by other changes in structure.[2] How might such compensation occur? The most obvious possibility is that the new cysteine residue might be geometrically positioned in such a way as to furnish a poor ligand for zinc. In view of the dimer−tetramer relationships noted above, a more subtle mechanism of compensation also appears to be worth considering.

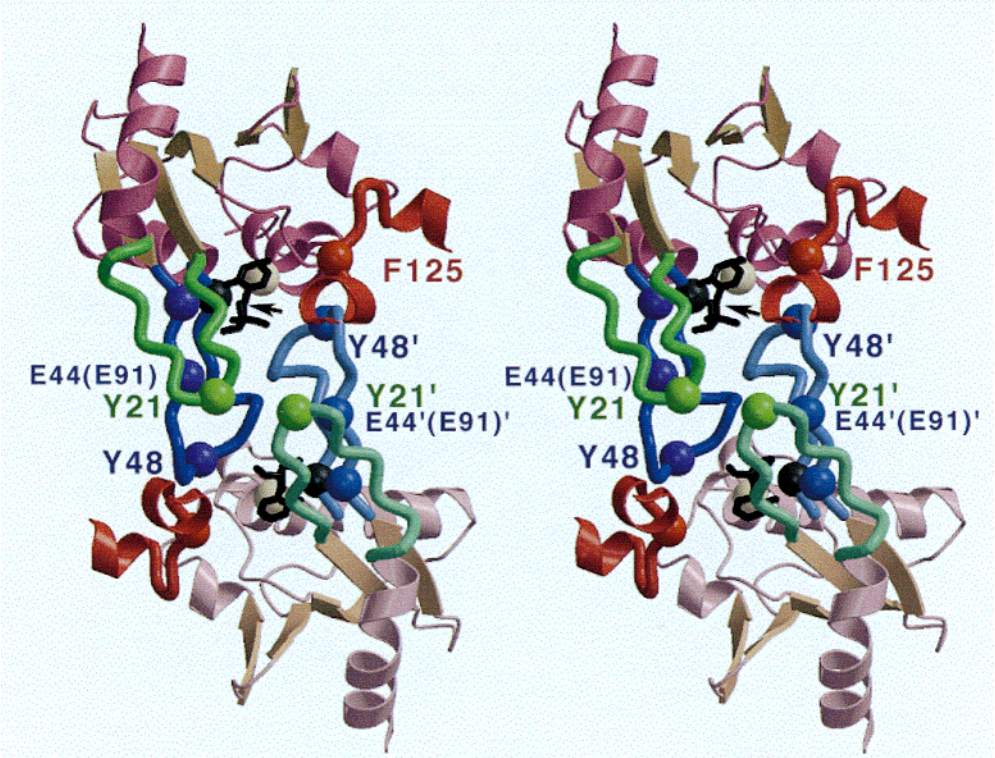

FIGURE 6: Schematic drawing in stereo of a novel interface in tetrameric cytidine deaminases, based on the approximate *222* symmetry in the *E. coli* enzyme. Two of the four subunits are shown in bold and pastel colors (primed residue numbers), the remaining dimer in the tetramer being generated using the exact 2-fold symmetry observed in the *E. coli* enzyme. Only the C-terminal portions of these two monomers are shown here (red). Loops from one monomer [*E. coli* residues 61−73 (green) and 88−103 (blue)] may provide tyrosine residues (*B. subtilis* residues Y23 and Y48), in trans, to complete the environment of aromatic side chains observed in the *E. coli* active site, as well as those interacting with the ribose. These residues are indicated by spheres at the position of the α carbon atoms. Colors are consistent with those used in Figure 2. In this model structure, Y48 is positioned close to the location of F233 in *E. coli.* Its hydroxyl group could therefore serve as a hydrogen bond donor to the third thiolate ligand at the position of the third cysteine zinc ligand, C53, as indicated by the arrow.

An important mechanism for modulating electronic properties of thiolate metal ligands is the use of NH-to-S hydrogen bonding. This mechanism is thought to underlie the varied behavior of iron−sulfur electron transport proteins by relative stabilization of the net charge on the prosthetic group (*26*, *27*). In the observed structure of the *E. coli* enzyme, one of the cysteine thiolate ligands (C129) receives H-bonds from two backbone amide groups, while the other thiolate ligand (C132) appears to adjust its zinc−sulfur distance as the negative charge on the nucleophilic oxygen atom varies during the course of the reaction (*28*). In the *B. subtilis* enzyme, with three sulfur ligands, the problem of excess negative charge is compounded. To solve that problem, it seems reasonable to suppose that the quaternary structure of tetrameric cytidine deaminases might instead furnish an additional proton *donor*, to decrease the negative charge on the third cysteinyl sulfur atom from C53 which takes the place of H102.

Substitution of tyrosine (Y48) for phenylalanine (F233) in the model described in the previous section provides a plausible hydrogen bond donor to the third cysteine residue (C53), as indicated by the arrow in the diagram. The active site construction for tetrameric CDAs, illustrated in Figure 6, thus provides all active site residues identified in the *E. coli* CDA with minimal alteration to the quaternary structure of the tetrameric CDAs. Contribution of key residues from each of three different monomers in the tetrameric quaternary structure could make the four active sites interdependent, in which case they could act cooperatively. We do not see evidence for such cooperativity in the measurements presented in Figure 3 (inset). Cooperativity may be subtle enough to evade detection by the crude, equilibrium Scatchard analysis presented here. On the other hand, our interpretation of the sequence conservation in terms conditioned by the approximate symmetry of the known *E. coli* CDA quaternary structure may be misleading. An alternate possibility is that the additional residues in the loop preceding the second group of zinc ligands serve as a "flap" covering the active site, in which case all four subunits may indeed act independently. To distinguish between these possibilities, it would be desirable to solve the crystal structure of a tetrameric cytidine deaminase.

[2] As a further illustration of the compensation effects that may be at work in the present comparisons, it is of interest that the dimeric cytidine deaminase of *E. coli* (with two cysteines and one histidine residue coordinating zinc in each subunit) and the monomeric mammalian adenosine deaminases (with three histidine residues coordinating zinc) were found to be similarly effective in transition state stabilization as indicated by the rate enhancement that each produces (*25*), and also similar in their affinities for transition state analogue inhibitors. These enzymes exhibit major differences in the nature of the overall protein fold, and even in such details as the chirality of the tetrahedral-like transition state that appears to be formed by covalent hydration of the substrate (*2*).

REFERENCES

1. Yang, C., Carlow, D., Wolfenden, R., and Short, S. A. (1992) *Biochemistry 31*, 4168−4174.

2. Betts, L., Xiang, S., Short, S. A., Wolfenden, R., and Carter, C. C. (1994) *J. Mol. Biol. 235*, 635−656.
3. Carlow, D. C., Smith, A. A., Yang, C. C., Short, S. A., and Wolfenden, R. (1995) *Biochemistry 34*, 4220−4224.
4. Smith, A. A., Carlow, D. C., Short, S. A., and Wolfenden, R (1994) *Biochemistry 33*, 6468−6474.
5. Vallee, B. L., and Auld, D. S. (1990) *Biochemistry 29*, 5467−5659.
6. Lipscomb, W. N., and Sträter, N. (1996) *Chem. Rev. 96*, 2375−2433.
7. Navaratnam, N., Morrison, J. R., Bhattacharya, S., Patel, P., Fanahashi, T., Giannoni, F., Teng, B. B., Davidson, N. O., and Scott, J. (1993) *J. Biol. Chem. 268*, 20709−20715.
8. Song, B. H., and Neuhard, J. (1989) *Mol. Gen. Genet. 216*, 462−468.
9. Laliberté, J., and Momparler, R. L. (1994) *Cancer Res. 54*, 5401−5410.
10. Vincenzetti, S., Cambi, A., Neuhard, J., Garattini, E., and Vita, A. (1996) *Protein Expression Purif. 8*, 247−257.
11. Miller, J. (1972) *Experiments in Molecular Genetics*, Cold Spring Harbor Laboratory, Cold Spring Harbor, NY.
12. Hanze, A. R. (1967) *J. Am. Chem. Soc. 89*, 6720−6727.
13. Carlow, D. C., Short, S. A., and Wolfenden, R. (1996) *Biochemistry 35*, 948−954.
14. Cohen, R. M., and Wolfenden, R. (1971) *J. Biol. Chem. 246*, 7561−7565.
15. Holmquist, B. (1988) *Methods Enzymol. 158*, 6−12.
16. Theirs, R. E. (1957) *Methods Biochem. Anal. 5*, 273−577.
17. Auld, D. S. (1988) *Methods Enzymol. 158*, 13−14.
18. Beaven, G. H., Holiday, E. R., and Johnson, E. A. (1995) *The Nucleic Acids* (Chargaff, E., and Davidson, J. N., Eds.) Vol. 1, pp 493−554, Academic Press, New York.
19. Frick, L., Yang, C., Marquez, V. E., and Wolfenden, R. (1989) *Biochemistry 28*, 9423−9430.
20. Peariso et al. (1998) *J. Am. Chem. Soc. 120*, 8410.
21. Bertini, I., Luchinat, C., Rosi, M., Sgamellotti, A., and Tarantelli, F. (1990) *Inorg. Chem. 29*, 1460−1463.
22. Keifer, L. L., and Fierke, C. A. (1994) *Biochemistry 33*, 15233−15240.
23. Christianson, D. W., and Fierke, C. A. (1996) *Acc. Chem. Res. 29*, 331−339.
24. Ippolito, J. A., and Christianson, D. W. (1994) *Biochemistry 33*, 15241−15249.
25. Frick, L., MacNeela, J. P., and Wolfenden, R. (1987) *Bioorg. Chem. 15*, 100−108.
26. Carter, C. W., Kraut, J., Freer, S. T., and Alden, R. A. (1974) *J. Biol. Chem. 249*, 6339−6346.
27. Carter, C. W. (1977) in *Iron−Sulfur Proteins*, Vol. III, pp 157−204, Academic Press, New York.
28. Xiang, S., Short, S. A., Wolfenden, R., and Carter, C. W., Jr. (1997) *Biochemistry 36*, 4678−4774.

BI990819T